Available online: http://journal.uir.ac.id/index.php/JEEE/index

Journal of Earth Energy Engineering

Publisher: Universitas Islam Riau (UIR) Press

Integrated Completion Study for Hpht Sour Gas Well Development In Carbonate Reservoir X

Steven Chandra[1], Wijoyo Niti Daton[1], Ellen Setiawan[1]
[1]Department of Petroleum Engineering, Faculty of Mining & Petroleum Engineering, Institut Teknologi Bandung, Jalan Ganesha No 10 Bandung, Indonesia, 40132
*Corresponding Author: steven@tm.itb.ac.id

Article History:

Received: June 18, 2021
Receive in Revised Form: September 12, 2021
Accepted: October 7, 2021

Keywords:

sour gas, corrosion, H_2S, CO_2, erosion, material selection

Abstract

The increasing need for energy sources and the decreasing available reserves have promoted oil and gas companies to explore and manage marginal reservoirs, such as the sour gaseous environment. This is to maintain the balance of energy supply and demand. Due to the supply of Natuna Gas Field, the gap in gas supply-demand is likely to decrease by 20%, as regards the example of a potential sour gaseous environment (Batubara, 2015). Therefore, the immediate development of this potential source is very relevant. The sour field approximately shares 40% of Indonesia's total gas reserve with 75% recovery, at an estimated OGIP of 222 TSCF. However, this environment is economically unproductive due to having high carbon dioxide (CO_2) and hydrogen sulfide (H_2S) contents, which are toxic and corrosive. Based on previous studies, the X-reserves reportedly contained 32% CO_2 and 7072 ppm H_2S, with fluid gravity of 42 API. This discretionary source of CO_2 was recently brought into production from a well with a depth of 8400 ft, perforated at a limited interval of 7100 to 7700 ft. The harsh environment presented many challenges to the completion of the design, as well as the need to incorporate corrosion effects with unique equipment and material selection for the tubular structure. Therefore, this study aims to determine reservoir fluids and production performance, as well as also predict the corrosivity of dissolved CO_2 in the natural gas. With the simulation and prediction, the proper material and equipment selection was obtained, based on the required sour service. The results showed that the wet gas reservoir of the X-field produced an optimum rate of 19.1063 MMSCFD. For the completion of the design, Nickel Alloy SM2535 or SM2242 was needed, due to damages in form of corrosion and pitting.

INTRODUCTION

Corrosion is the destructive attack of materials through environmental reactions and other natural potential hazards associated with oil/gas production and transportation. This occurs because of three elements, namely the anode, cathode, and electrolyte. The anode is a site of corroding metal, while the cathode creates an electrical conductor during the process of corrosion. However, the electrolyte is a corrosive medium aiding the transfer of electrons from the anode to the cathode. Moreover, a sour gas environment contains various high-impurity and corrosive products. In this environment, such as well and pipelines, the highly corrosive components observed are carbon dioxide (CO_2), hydrogen sulfide (H_2S), and free water. The continuous extraction of these components through hydrocarbon is found to ensure the stress of the internal surfaces from the effects of corrosion. This indicates that the lines and component fittings are likely to cause material degradations, due to changes in fluid compositions, souring of wells, as well as the operating conditions of the pressures and temperatures.

The results of these degradations in the loss of mechanical properties such as thickness reduction and failure lead to complete breakdown and replacement needs while production is stopped. Therefore, the

DOI: 10.25299/jeee.2022.7133
eISSN: 2540-9352 pISSN: 2301-8097

Journal of Earth Energy Engineering
Vol. 11 No. 1, March 2022, pp 34-51

serious consequences of this corrosion process are one of the most important problems in the oil and gas industry. To handle this challenge, the expected corrosion rate has to adopt technical solutions, which causes low risk or accepted reliability. This leads to the fabrication of a specialized completion material design with a high percentage of tubular goods, as well as carbon steel and alloy. In this case, X-Field has reportedly been investigated based on gas composition, partial pressure, and the concentration of corrosive agents. Furthermore, the X-Field reservoir is a gas storage with 66% methane, 7072 ppm H_2S, and 32% CO_2. Since the field has been categorized as a sour environment, predicting the corrosion models and selecting appropriate tubular materials are very essential, to develop an ideal plan for the reserve. Therefore, the most effective plan is achieved to maintain production economically.

Objectives of the Study

This study aims to,

1. Determine reservoir fluid types and properties.
2. Construct the IPR and VLP matching model, to estimate production performance.
3. Determine the corrosion and erosion damage prediction, as well as compare the results with several standard allowances.
4. Create a completion design for tubing material selection, based on the results and considerations.

Basic Theory

A natural gas containing more than 4 ppm of hydrogen sulfide (H_2S) is often known as being "sour" (Boschee, 2014). This is because the significant quantities of these global gaseous resources are known to contain H_2S. These have been previously difficult to produce due to causing corrosion and sulfide stress cracking, especially in pipelines (Singh, 2010). The NACE Standard MR0175-881 provides several guidelines in defining a sour environment, for the general selection of carbon and low alloy steels. These definitions showed that the 0.05 psig (0.34-kPa) H_2S partial pressure in the gas phase was considered as “sour”. Also, the possibility for sour service conditions should be evaluated during this lifetime. This service is defined according to the EFC Publication No. 16 for carbon steel, as well as NACE MR0175 for CRAs and Titanium alloys. The requirements for metallic materials in the sour service should also comply with this standard. Additionally, the use of corrosive inhibitors should not relax the requirement based on using the service resistant materials when the conditions are categorized as "sour" by the above standard.

According to the oil and gas industry, there are two agents of corrosion in the sour field, namely hydrogen sulfide (H_2S) and carbon dioxide (CO_2) (Popoola et al., 2013). The corrosion reactions for these two gases are dependent on water, leading to severe pitting or metal loss in the form of uniform thinning. Apart from reacting with iron and causing metal loss, the presence of CO_2 causes the formation of an acid that lowers pH and accelerates the H_2S corrosion reaction. Moreover, CO_2 corrosiveness is specifically harmful in high velocity/high-pressure environments, leading to increased pitting rates caused by a combination of corrosion and erosion (Kilstrom, 1983). The rate of corrosion is also calculated in mils or millimeters per year (MPY, mm/yr or MMY). Based on Pots et al., (2002b), a mechanistic equation was modeled for predicting CO_2 corrosion. This focused on electrochemical studies, to show the correlation between temperature (°C), CO_2 partial pressure, and corrosion rate (mm/yr). The equation for this CO_2 corrosion rate is shown as follows (Dugstad experimental, 1994),

$$\log(CR_t) = 5.8 - \frac{1710}{T + 273} + 0.67 \log\left(P_{CO_2}\right) \dots (1)$$

When selecting the right metal for completion design, several factors are needed for consideration, based on the materials selection process reflecting the overall design life, cost profile, maintenance and safety, and other specific project requirements (Singh, 2010). This selection should be optimized, as well as provide acceptable safety and reliability. At a minimum standard, the following should be considered,

- Corrosivity, based on specified operating conditions including start-up and shut-down conditions,
- Design life and system availability requirements,
- Failure probabilities, modes, and consequences for human health, environment, safety, and material assets,
- Resistance to brittle fracture,
- Inspection and corrosion monitoring,
- Access for maintenance and repair.

Several methods are found to be available in combating the corrosive attack of sour gas. In this case, corrosion-resistant alloy (CRA) is selected for material selection due to the occurrence of a corrosive environment. This material includes carbon, stainless, and alloy steels, respectively. As proposed by (Smith, 1999), the applicable CRA in the oil and gas industry includes 13Cr, Super 13Cr, 22 and 25Cr

duplexes, 28Cr stainless steel, as well as 825, 625, 2550, and C276 Nickel Alloys. With highly partial pressure of carbon dioxide and low pH, alloy steel is more considerable than other categories (Papavinasam, 2014).

According to Fig 1, alloy steel has additional chemical elements to improve certain properties. Some of the most common elements are manganese, nickel, chromium, molybdenum, vanadium, silicon, and boron. These materials are subsequently split into two categories, namely low and high alloy steels. The low materials have less than 8% compositional elements with better hardness and resistance to wear over carbon steel, although possess less tensile strength. Meanwhile, the high alloy steels have more than 8% compositional elements with better properties than the low materials (Dr. Fatih Birol, 2019).

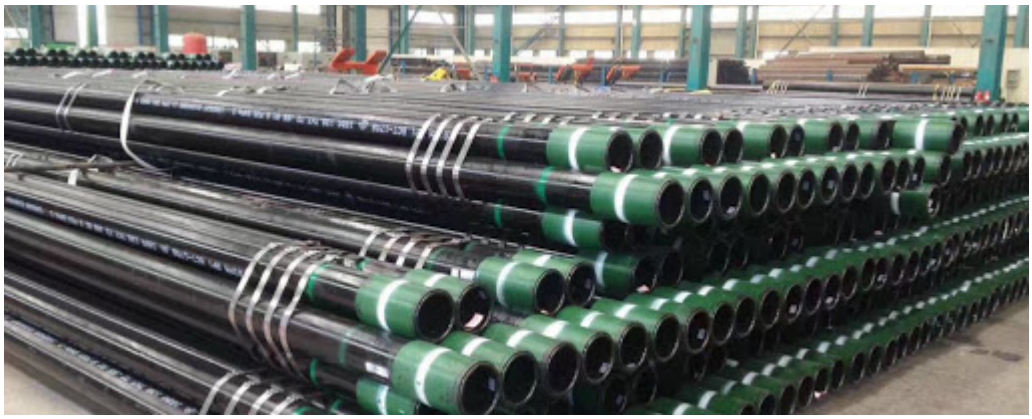

Source: Sumitomo Metal SM2535
Figure 1. Corrosion resistant alloy pipes for sour gas environment

METHODS
This study was conducted through several steps, where a flowchart explained the methodology of the whole experiment, as shown in Fig 2 and these steps are as follows:

1. Data acquisition
   The reservoir fluids composition, storage condition (pressure and temperature), DST and CCE tests, as well as a complete design, were obtained and used as input parameters in the corrosion rate and erosional velocity prediction.

2. Fluid properties analysis
   Based on gas composition, the fluid types were obtained using a Constant Composition Expansion (CCE) method with PVTp software. Fluid properties such as gas deviation (z), viscosity, and formation volume factors, were constructed after the CCE matching.

3. IPR and VLP model construction
   This model was constructed by considering the previous fluid properties and DST test, using the PROSPER software. Subsequently, the best correlation for VLP/IPR matching was determined, leading to the operating point as optimum production range. In addition, sensitivity analysis was created for top node pressure, ranging from the reservoir to abandonment pressure.

4. Corrosion and erosion rate prediction
   The input parameters for corrosion and erosion rate prediction contained wellhead and bottom-hole conditions, DST gas composition, water chemistry, flowrate, and wellbore angles in the ECE (Electronic Corrosion Engineer) software. This subsequently led to a damaged rate and alloy tubing evaluator.

Journal of Earth Energy Engineering
Vol. 11 No. 1, March 2022, pp 34-51

5. Tubing material selection
   The final material selection for tubing was considered based on the ISO 15156-3 standard and Nippon Steel chart, including temperature, as well as CO_2 and H_2S partial pressures.

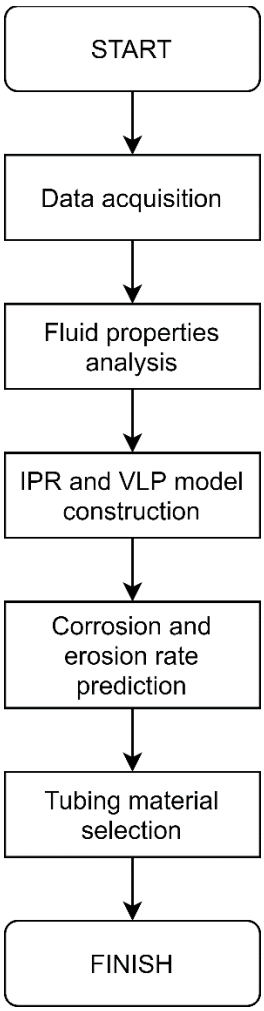

Figure 2. Workflow of the Research

Several assumptions were also used in this study: (1) The conditions of pressure and temperature remained constant along the pipeline, and (2) The constant rate and fluid composition during production, where the wellbore was assumably installed vertically on the ocean (measure depth equals to true vertical depth) while neglecting pressure losses due to friction. Also, the size of the borehole used the general assumption of 7 and 5 inches, respectively for casing and tubing with depth of tubing was precisely considered above top perforation. Based on the assumptions of the pipe to bear the damage rate occurrence, no change was expected during the estimated design life. Consequently, the need for corrosion mitigation methods, such as inhibitor, was not required.

Case Study

At the beginning of the production, the X-field produced at the formation had a perforated interval from 7100 to 7700 ft (Fig 3). Also, the reservoir fluid composition mainly contained 66% methane, 32% CO_2, 7072 ppm H_2S, 3308 psi pressure, and 211°F temperature, as shown in Table 1. Furthermore, the samples were transferred to a PVT lab, where several tests and measurements were conducted using the Constant Composition Expansion (CCE) method (Table 2). The PVT matching and initialization procedure with the test data was also performed for the fluid, based on the compositional model. In this case, the constructed fluid properties models were gas deviation (z), viscosity, and formation volume factors, respectively.

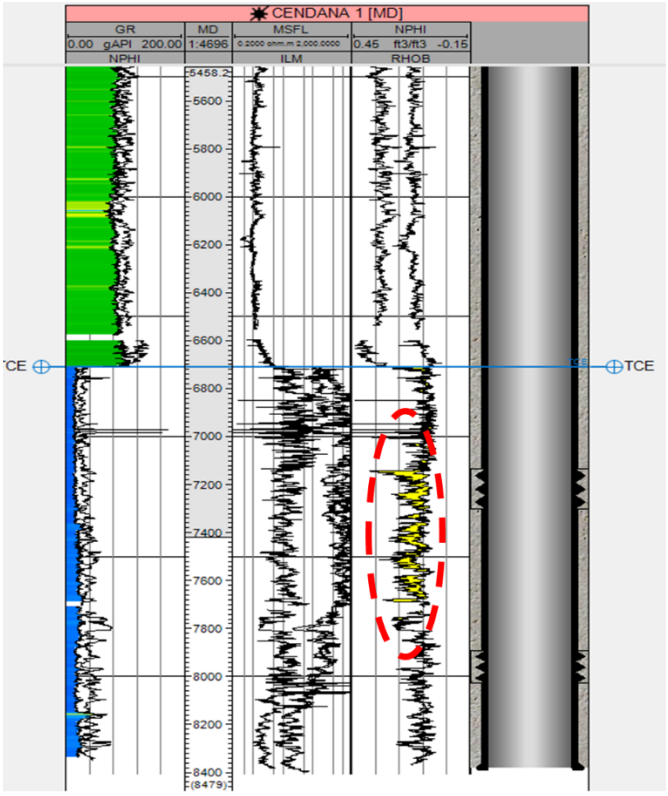

Figure 3. Perforation interval – completion design

Table 1. Fluid composition

Component	Mol %		
	Separator Liquid	Separator Gas	Well Stream
Hydrogen Sulfide	0.2	0.43	0.43
Carbon Dioxide	4.68	27.98	27.94
Nitrogen	0.01	0.41	0.41
Methane	5.48	66.5	66.4
Ethane	0.93	2.72	2.72
Propane	0.9	0.94	0.94
Iso-Butane	0.41	0.2	0.2
N-Butane	0.78	0.29	0.29
Iso-Pentane	0.45	0.08	0.08
N-Pentane	0.54	0.08	0.08
Hexanes	1.43	0.08	0.08
Heptanes	7.94	0.19	0.2
Octanes	10.42	0.07	0.09
Nonanes	11.42	0.02	0.04
Decanes	9.73	0.01	0.03
Undecanes Plus	44.68	0	0.07

Journal of Earth Energy Engineering
Vol. 11 No. 1, March 2022, pp 34-51

Table 2. CCE – PVT tests

PRESSURE VOLUME RELATIONS (at 311F)			
Pressure	Relative Volume	Liquid Volume Percent	Deviation Factor Z
6000	0.4172		1.034
5600	0.495		1.014
5200	0.5231		0.995
4800	0.5567		0.978
4400	0.5976		0.963
4000	0.6483		0.95
3800	0.6783		0.944
3400	0.7505		0.935
3325	0.7663		0.934
2900	0.8723		0.928
2800	0.9023		0.927
2700	0.9347		0.926
2600	0.9698		0.925
Pd=2520	1	0	0.925
2400	1.0195	Trace	
2300	1.095	Trace	
2200	1.145	Trace	
2100	1.2		
1900	1.3283		
1700	1.4883		
1430	1.7779		
1265	2.0172		
1132	2.2615		
1026	2.5019		
952	2.7016		

Based on the simulation, a nodal analysis was then carried out using the PROSPER software, to determine the operating rate of the reservoir, due to the stabilized data from the DST #2 test (Table 3). From DST #2, the data were further used for determining the C and n-value, to construct the IPR curve based on Rawlin's correlation. Additionally, the operating point was determined by creating a VLP/IPR curve. A gray correlation was selected due to being suitable for the gas reservoir and having the smallest standard deviation.

Table 3. DST #2 tests

Flowrate	Gass (MMSCFD)	Oil (BOPD	Water (BWPD)	BHP (psia)	WHP (psig)	WHT (F)
1	21.5	54	84	3089	1265	190
2	16.6	44	59	3148	1820	198
3	11.2	40	70	3242	2426	192

The corrosion and erosion model prediction were also conducted using the ECE (Electronic Corrosion Engineer) software, which helps in calculating the rate of corrosiveness based on the modified technique developed by de Pots et al., (2002b). Moreover, the ECE proposed a corrosion prediction expression, using corrosive reactions and mass transfer effects, which represented the main part of the dependence on flow velocity and pipe diameter. This software also developed corrosion prediction by involving several variables, such as gas composition, bottom-hole and wellhead conditions, water chemistry, flowrate, well and deviation. Conclusively, the material selection for tubing was considered based on the ISO 15156-3 standard and Nippon Steel chart, including the CO_2 and H_2S partial pressures.

RESULT AND DISCUSSION

1. PVT Analysis

Fluid samples were obtained from well X and subsequently transferred to a PVT lab, where several tests and measurements were conducted by chromatography. From these data, two DST tests were obtained from different intervals as follows:

- Interval 2175 – 2225 m, where DST #2 was selected because the reservoir limit showed a bigger production rate and was also thicker (based on NPHI-RHOB log).
- Interval 2406 – 2447 m.

Several methods were also used for quality validation, namely the Hoffman plot, mass balance test, and the liquid drop-out data. The Hoffman plot was used to validate and evaluate the quality of the compositional data, employing a log-linear plot of K-value versus Hoffman factor for the recombination process of condensate (liquid and vapor compositions) (Lawrence & Gupta, 2009). However, the composition in this study focused on wet gas, which was unable to be validated with the Hoffman plot. Also, the available data was only the Constant Composition Expansion (CCE), while the liquid drop-out parameters required both the CCE and CVD (Constant Volume Depletion) results.

Based on this study, the CCE method was used, by firstly applying the CVD to characterize the reservoir fluid, such as the retrograde condensate and volatile oil. In the composition data, the reservoir fluid obtained was a wet gas, because most of the components observed were C_1, at approximately 66%. Secondly, further tests were not needed to determine the fluid composition, due to the data already showing the components. Thirdly, the CCE test was performed to determine fluid characteristics and properties, such as gas viscosity, FVF, and z-factor. Meanwhile, the CVD test was carried out for advanced measurements, such as the recovery of original positions and retrograde condensation accumulation. From the CCE test, the relative volume of the fluid was measured, leading to the determination of the fluid properties' values.

A phase diagram is one of the tools used to determine the reservoir fluid type. The combination of this diagram and the fluid properties obtained from the sample was matched with the PVT data test. From the constructed phase envelope (Fig 4a), the results are shown in Table 4, where the diagram from the sample has a cricondentherm and cricondenbar of 430.3°F and 3050.7 psig, respectively. Also, the reservoir temperature and pressure were 211°F and 3293.3 psig. Therefore, the reservoir path should be outside the phase diagram. This subsequently indicated two types of storage fluid, namely, wet and dry gases.

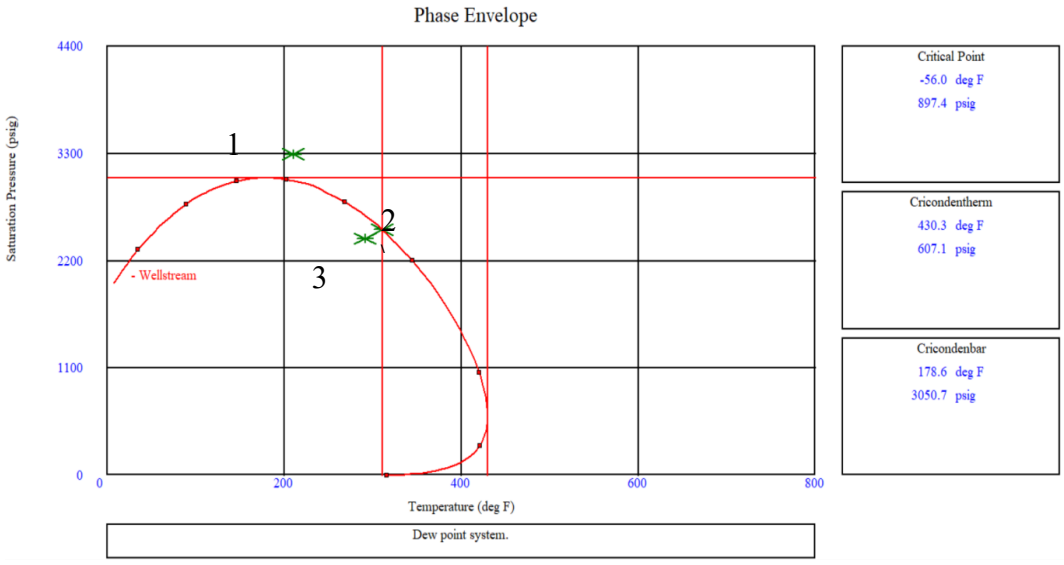

Where 1 is reservoir path, 2 is dew point pressure, and 3 is separator point.

Figure 4a. Phase envelope of the sample (PVTp software)

Journal of Earth Energy Engineering
Vol. 11 No. 1, March 2022, pp 34-51

Table 4. Phase envelope results

No.	Component	Value
1	Critical Temperature (F)	-56
2	Critical Pressure (psig)	897.4
3	Cricondentherm (F)	430.3
4	Cricondenbar (psig)	3050.7
5	Dew Point Pressure (psig)	2511.842 (with error of 0.324% regarding PVT test)

Based on this study, the separator condition was 2426 psig and 192°F, which were within the phase diagram. Therefore, the sample was wet gas, as shown in Fig 4a (compared to the theoretical wet gas envelope from McCain in Fig 4b). This was confirmed by the liquid component in the separator condition, which was much bigger compared to the well-stream point (Table 1). Besides that, the fraction of methane was 66.4 %, with the GOR bigger than 50,000 SCF/STB and this indicated the wet gas fluid type. Figures 5-7 show the fluid models (z, μμ, and Bg) of the sample.

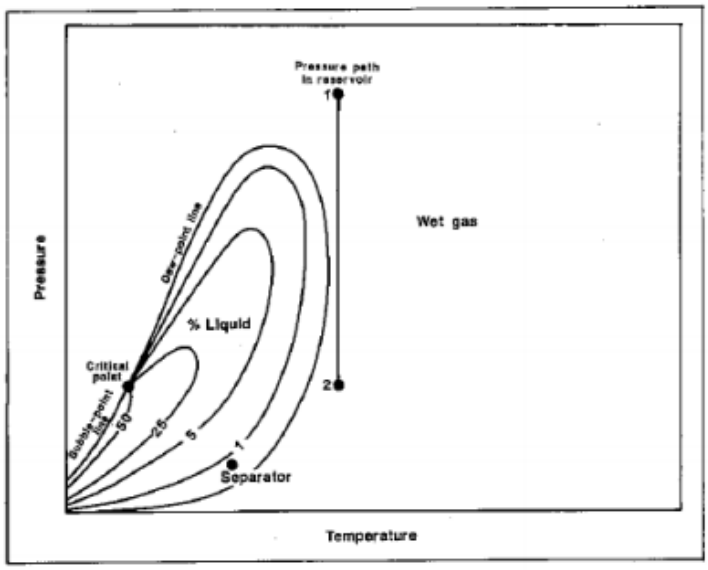

Figure 4b. Theoretical phase envelope of wet gas (McCain, 1990)

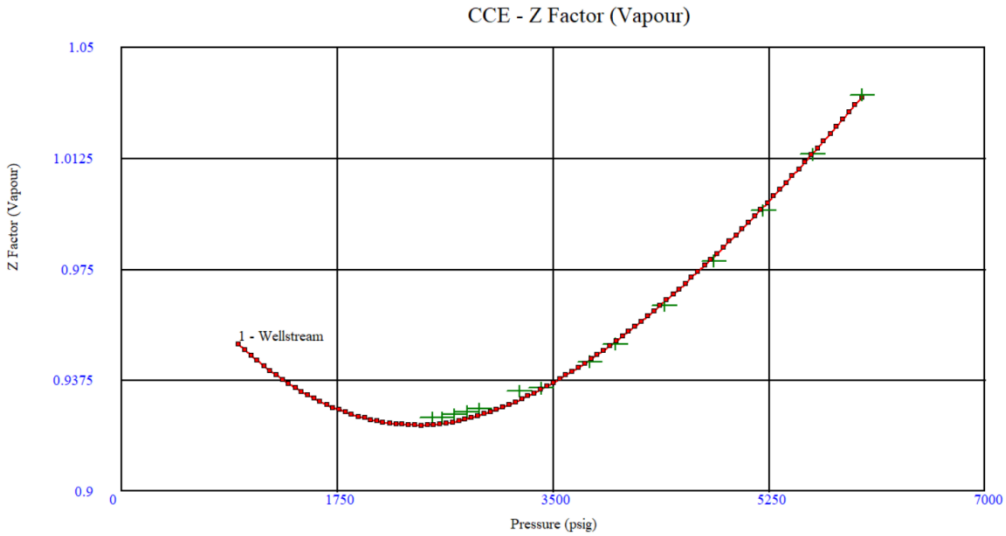

Figure 5. Gas deviation factor (z) of the sample

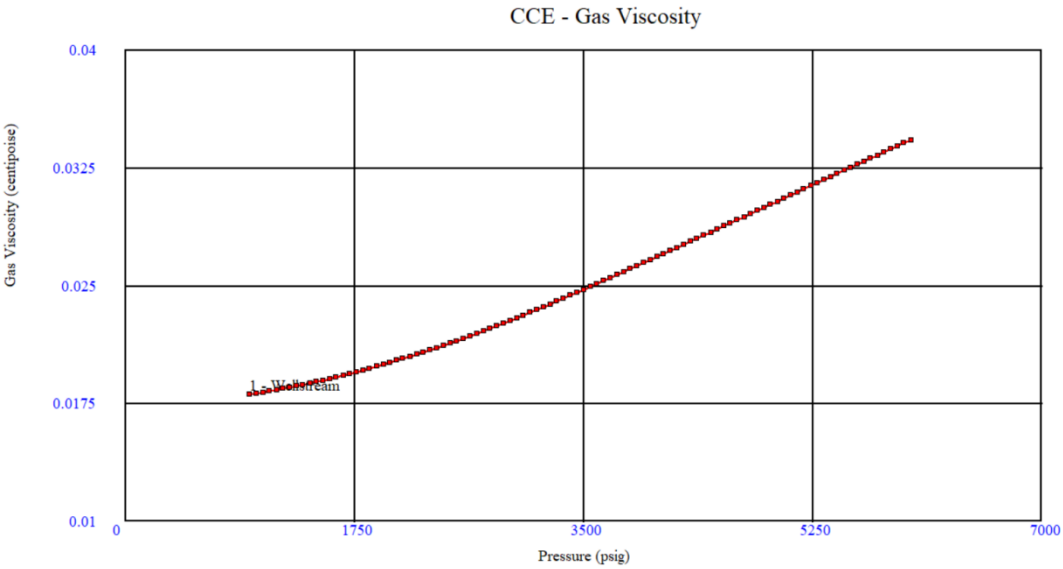

Figure 6. Gas viscosity of the sample

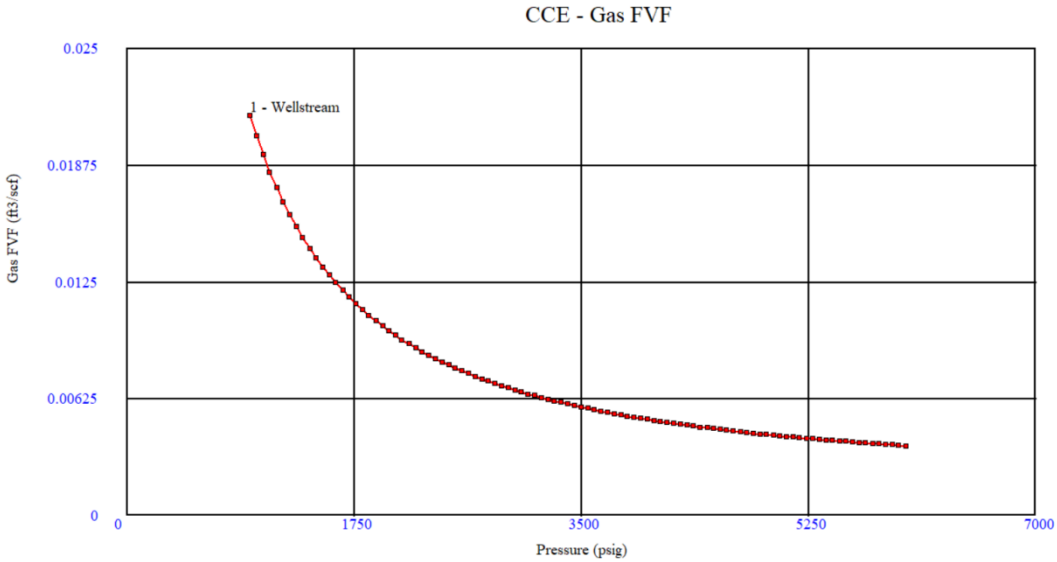

Figure 7. Gas formation volume factor of the sample

2. Production Forecast and Optimum Production Range

The inflow performance relationship (IPR) curve was created by using the C and n-method from Rawlin's correlation with three DST #2 data. By plotting ΔP2 vs. q on a log-log graph (Fig 8), the best trendline function was produced through the data points with n and C-value of 0.5445 and 8.82132, respectively. The IPR curve was also compared to other graphical representations, using only two data (Fig 9). From the curve, the absolute open flow (AOF) value was observed to be 59.648 MMSCF/D. Besides that, the inputted test data points were matched with the constructed IPR curve, as shown in Fig 10.

Journal of Earth Energy Engineering
Vol. 11 No. 1, March 2022, pp 34-51

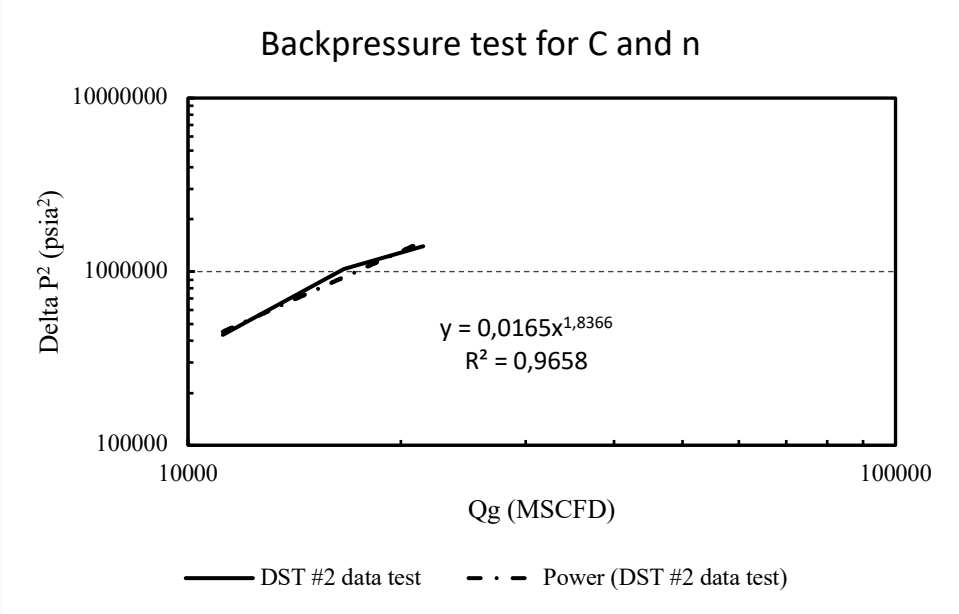

Figure 8. Backpressure test for C and n

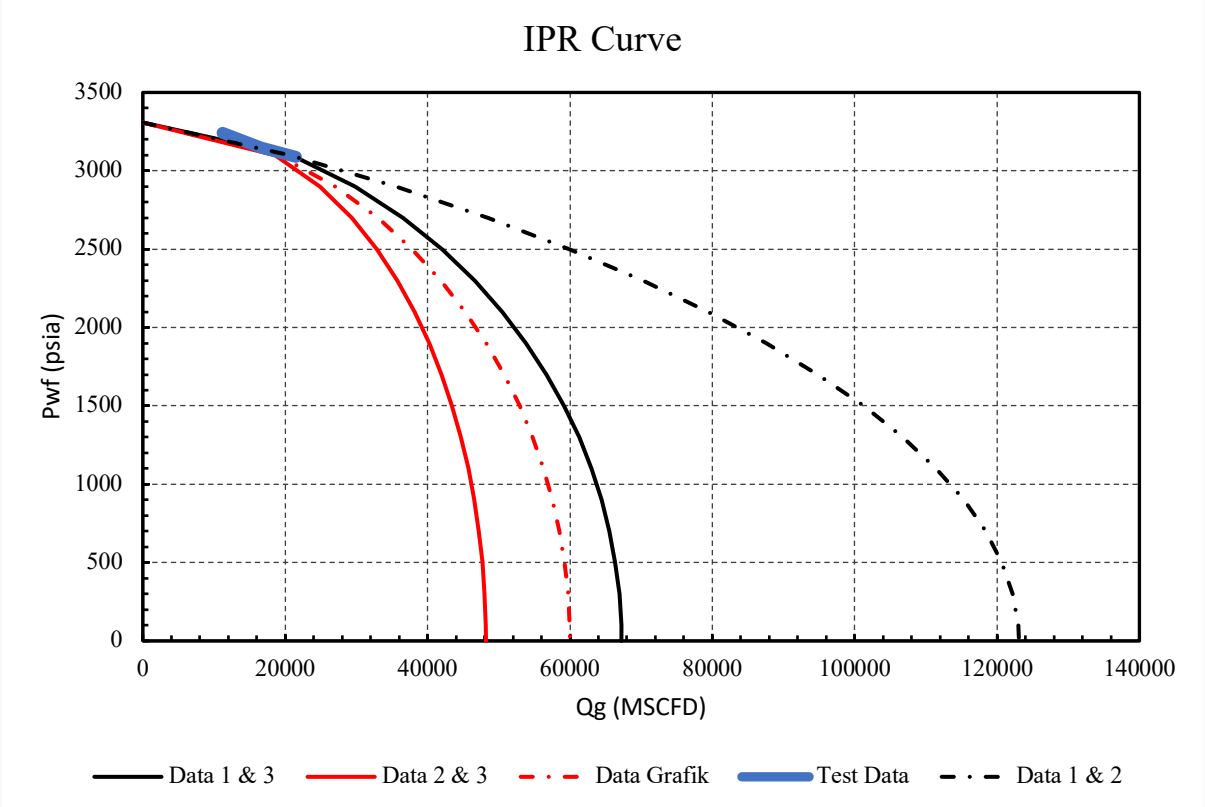

IPR curves above are created with only using two data from DST #2 test (i.e. Data 1&3 means the C and n value are calculated from flow periods 1 and 3 from DST #2).

Figure 9. IPR curve with different test data

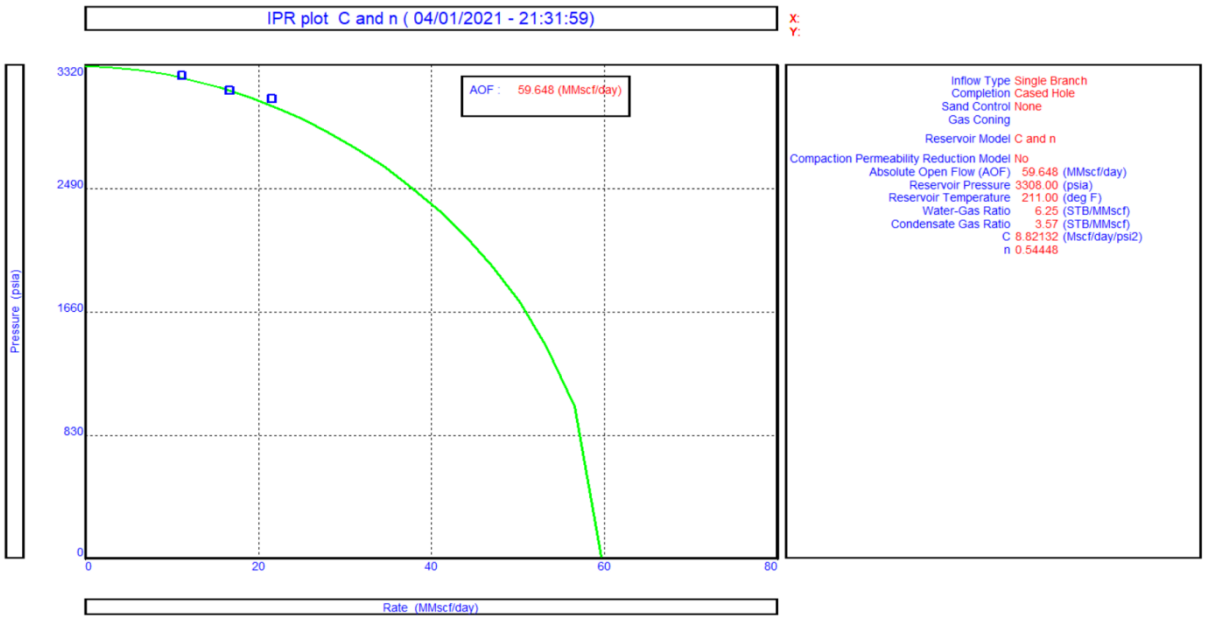

Figure 10. IPR with matched test data (PROSPER software)

There was the need to create a VLP-IPR matching with the existing data after creating the IPR curve, to determine the operating point. This was based on determining the most fitted and proper correlation in the VLP sensitivity analysis. With the guidance for each available correlation, only several associations were used for the VLP matching (Francher Brown, Duns and Ros, Gray, Beggs and Brill, as well as Petroleum Experts) with the fluid and reservoir characteristics. Therefore, the value of standard deviation for all correlations is shown in Figure 11.

TUBING CORRELATION MATCH PARAMETERS (IPR_revisi (C and n dari grafik log-log).Out)

Done | Cancel | Main | Reset all | Report | Export | Help

		Correlation	Parameter 1	Parameter 2	Standard Deviation
1	Reset	Duns and Ros Modified	1	1	
2	Reset	Hagedorn Brown	1	1	
3	Reset	Gray	0.23288	25.0971	41.8328
4	Reset	Mukerjee Brill	1	1	
5	Reset	Beggs and Brill	0.82331	41.287	72.2287
6	Reset	Petroleum Experts	0.23288	25.0971	41.8328
7	Reset	Orkiszewski	1	1	
8	Reset	Petroleum Experts 2	0.23288	25.0971	41.8328
9	Reset	Duns and Ros Original	1.12578	1	790.452
10	Reset	Petroleum Experts 3	0.23288	25.0971	41.8328
11	Reset	GRE (modified by PE)	1	1	
12	Reset	Petroleum Experts 4	1.55514	0.2	871.064
13	Reset	Hydro-3P	1	1	
14	Reset	Petroleum Experts 5	1.1655	44.8897	205.005
15	Reset	OLGAS 2P	1	1	
16	Reset	OLGAS 3P	1	1	
17	Reset	OLGAS3P EXT	1	1	

Figure 11. Tubing correlation statistic results

To select the correct correlation in the VLP sensitivity analysis, the smallest standard deviation value was observed between the correlations and further supported by the difference in each correlative value. Furthermore, the Gray correlation provided good gas well results for high water and condensate ratios, at approximately 50 BBL/MMSCF. The standard deviation and the value difference of this correlation were

Journal of Earth Energy Engineering
Vol. 11 No. 1, March 2022, pp 34-51

the smallest, compared to other associations. This was suitable for the gas reservoir and had advantages in the quick calculation. Therefore, a Gray correlation was used for VLP/IPR matching (Fig 12).

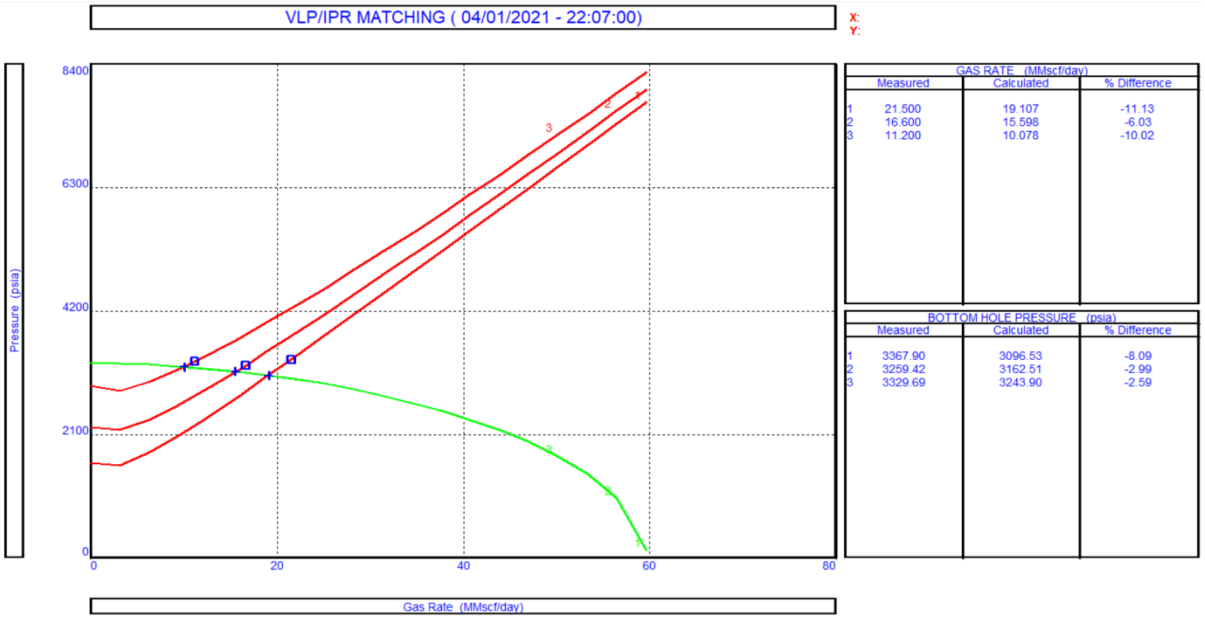

Figure 12. VLP/IPR matching

The maximum and minimum value boundaries were water coning and liquid loading/economic limit for gas well optimum rate, respectively. In this case, the boundary limits for optimum production range were calculated using the thumb rule method of 30 – 70% of AOF (17.89 MMSCFD – 41.754 MMSCFD) technique. Therefore, the operating point was 19.1063 MMSCFD (Fig 13).

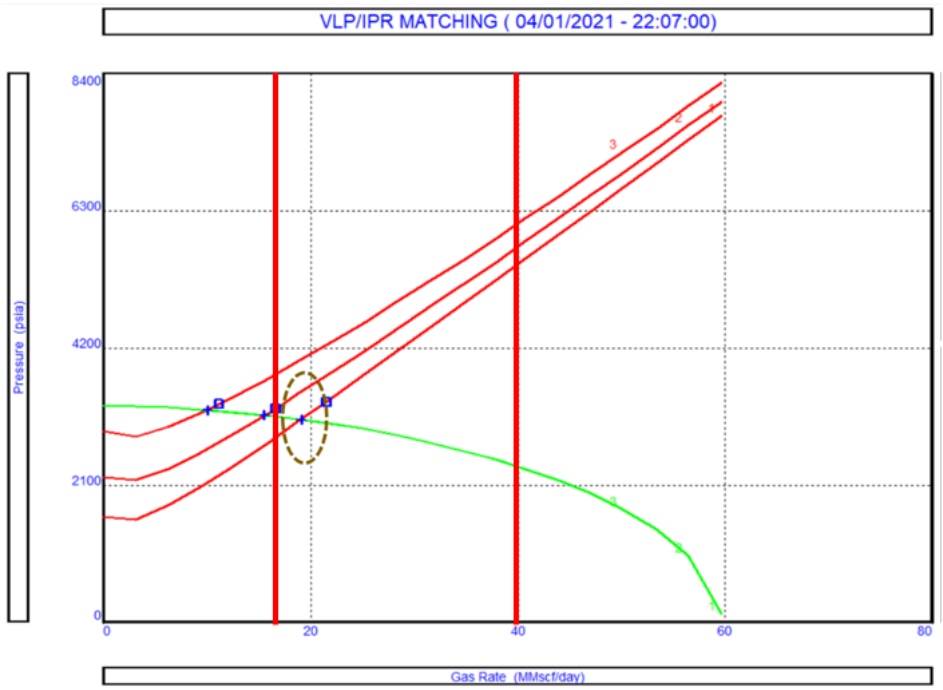

Figure 13. Optimum production range with operating point

Based on this study, a top node was used as a solution in sensitivity analysis, which was shown for reservoir pressure parameter from the initial value to abandonment pressure (assumed 300 psi), in Fig. 14 and 15.

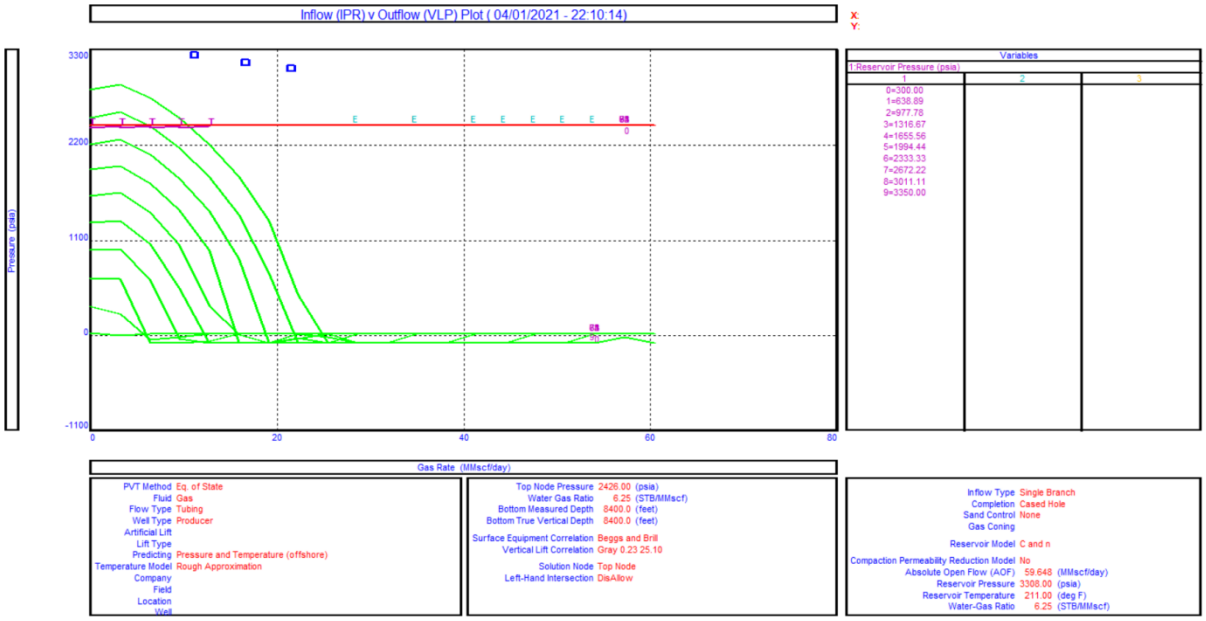

Figure 14. Sensitivity analysis – system plot

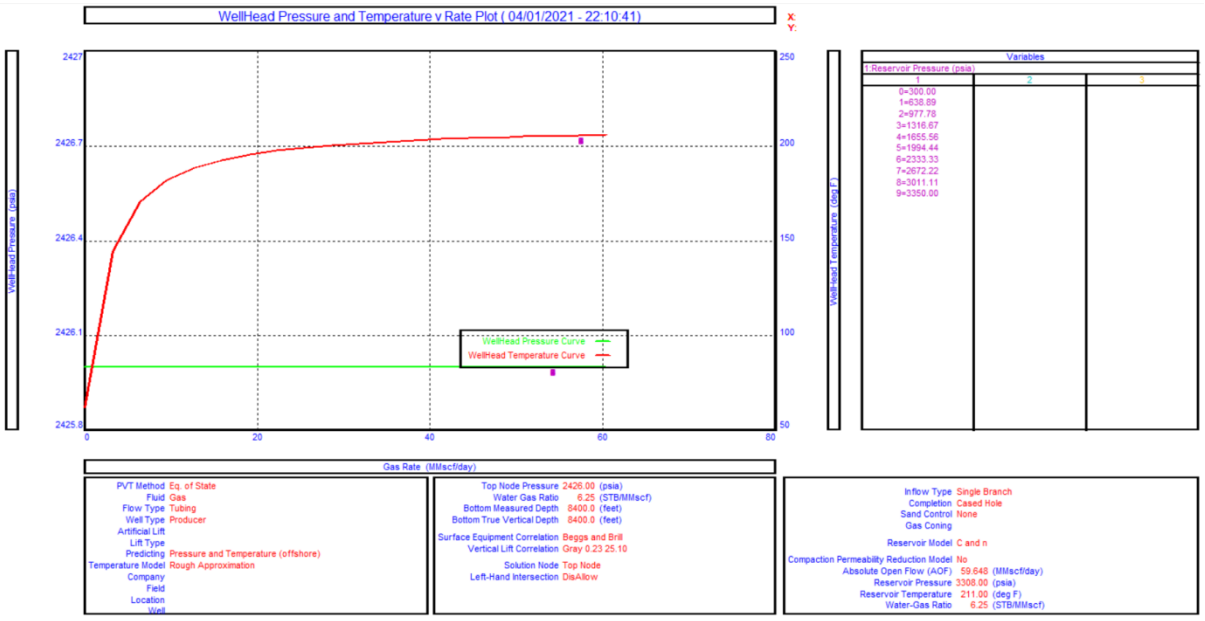

Figure 15. Sensitivity analysis – wellhead plot

3. Corrosion Rate and Allowance

The damage rate of both corrosion and erosion was predicted using the ECE (Electronic Corrosion Engineer) software with the data of flow period 3 from DST #2. The composition for CO_2 and H_2S was also obtained using the DST #2 as the bottom-hole condition, which was initially contacted with the wellbore flowing rate. However, when using well-stream data, several adjustments were observed in the surface, changing the fluid composition. Additionally, the API RP 14E introduced the empirical erosional velocity equation shown as follows:

$$V_c = \frac{c}{\sqrt{\rho_m}} \ldots (2) V_c = \frac{c}{\sqrt{\rho_m}} \quad (1)$$

Journal of Earth Energy Engineering
Vol. 11 No. 1, March 2022, pp 34-51

V_cWhere, V_c = the fluid erosional velocity in ft/s, c = the empirical constant in $\sqrt{\frac{lb}{ft\,s^2}}\sqrt{\frac{lb}{ft\,s^2}}$, and $\rho_m\rho_m$ = the gas/liquid mixture density at flowing pressure and temperature in lb/ft^3. Furthermore, the selection of cc is shown in Table 5, where continuous service is observed with the tubing material for X-Field being corrosion resistance alloy. Therefore, $c$the c factor was selected to be 150. Fig 16 and Table 6 also show the corrosion-erosion rate prediction, with Fig 17 showing that the risk of failure occurred during operational times.

Table 5. Suggested c factor (API RP 14E)

Fluid			Suggested c-factor	
			Continous Service	Intermittent Service
Solid-free		Non-corrosive		
		Corrosive + Inhibitor	150-200	250
		Corrosive + CRA		
		Corrosive	100	125
	With solids		Determine form specific applications studies	

Table 6. Damage rate prediction results

Corrosion rate (mm/year)	Erosion rate (mm/year)	Maximum isolated pitting (mm/year)	Sour Service
0.46	0	4.5	Yes - Region 3 (according to ISO 15156-3)

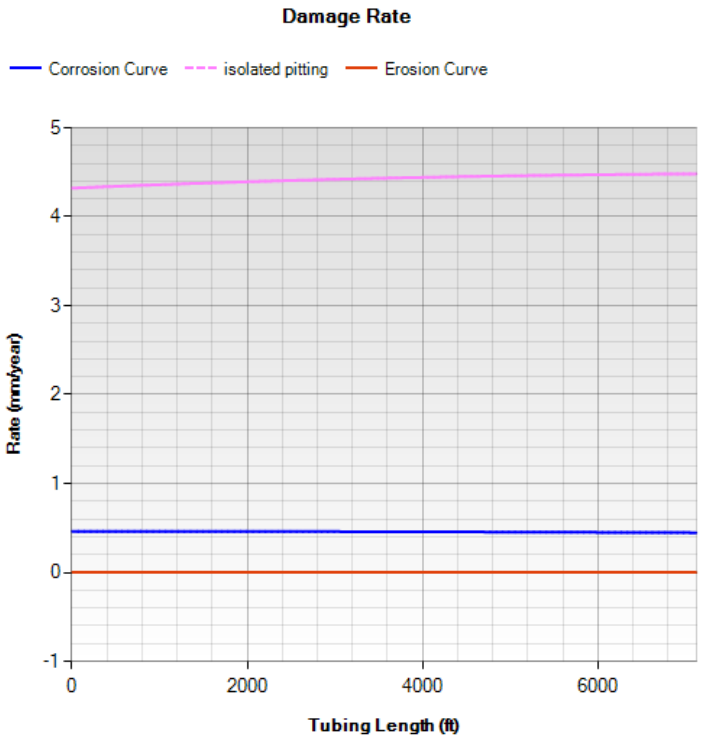

Figure 16. Damage rate prediction (ECE software)

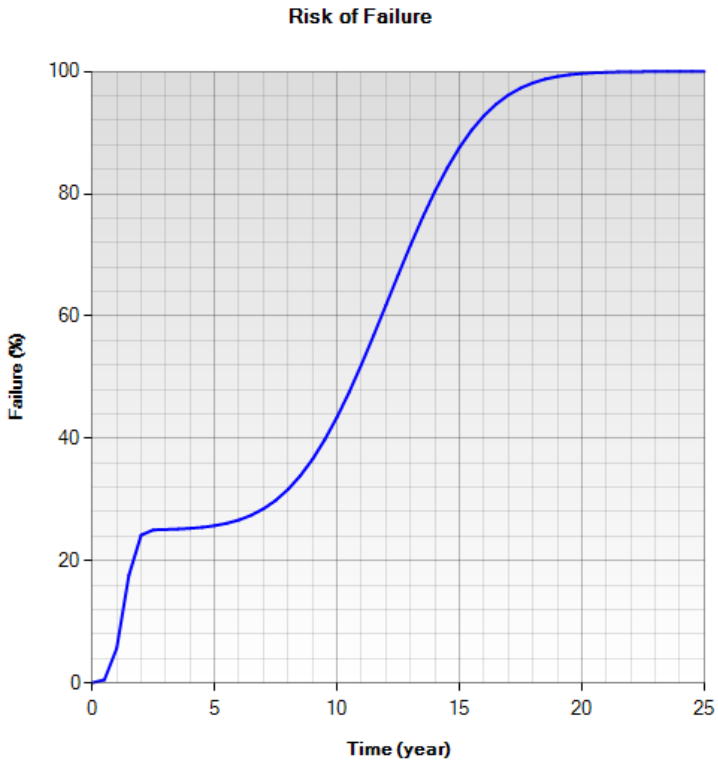

Figure 17. Risk of failure

The graphs of corrosion and erosion showed the methods by which the rate of occurrence in the pipes was annually reviewed. From this graph, the option of using thick/corrosion-resistant alloy or non-CRA pipes was evaluated, subsequently affecting the material selection and cost. According to Table 6, the maximum value of corrosion was 0.46 mm/year, with a significant partial pressure of CO_2. Also, pipe failure was more than 40% in the 10th year, which was found to be continuously increasing yearly. This indicated that the pipe should be changed from the 10^{th} year of operation. Pitting corrosion of 4.5 mm/year was also observed, which was a localized form of corrosiveness where cavities or "holes" were produced in the material (Dugstad et al., 1994). Moreover, a small and narrow pit with minimal overall metal loss led to the failure of an entire engineering system. From the simulation, sour service (Region 3) implies high H_2S condition (22.927 psi) combined with low pH or severe conditions (NACE MR0175/ISO15156-3). To ensure the acceptability of the tubing corrosion rate, several standards such as NACE paper 02235 (Pots et al., 2002a) and (Norsok & Industries, 2002), are shown in Table 7. In addition, tubing was further categorized as piping in NACE standard, as the rate of corrosion should not exceed 6 mm/year. This indicated that the maximum corrosion rate for tubing in the X-Field was 0.46 mm/year. Therefore, this process was safe, with the ability to provide good well integrity during the production stage.

Table 7. Corrosion allowance standards

No	NACE (Paper 02235, 2002)	NORSOK (Paper M-001, 2002	CO2 Partial Pressure
1	< 8 mm/year for pipeline	Corrosion allowance = (design life - x years) * 0.4 mm/year	0-3 psi: very low-non chrome use possible
2	< 6 mm/year for piping	For carbon steel and SMI3Cr: 2-12 mm/year	3-7 psi: marginal for chrome use
3	< 3 mm/year for vessel	For stainless steel: 12 mm/year	7-10 psi: medium to serious problem

According to the NORSOK standard, the acceptable corrosion rate was 2 – 12 mm/year, since the tubing material was CRA. This was found to be below the limit, indicating that the tubing was safe with the ability to provide good well integrity. Also, the chrome usage was determined from the partial pressure of CO_2, which was observed at 1037.44 psi. This was considered a serious problem, and CRA was necessary.

Journal of Earth Energy Engineering
Vol. 11 No. 1, March 2022, pp 34-51

4. Tubing Material Selection

From the tubing material selection, the results are obtained in Table 8 using several evaluation rules for specification (ECE results, ISO 15156-3, and Nippon steel chart).

Table 8. Summary of tubing material selection after simulation

ECE Simulatio Results	ISO 15156-3 Evaluation Rules	Nippon Steel Material Chart
Alloy (28, 825, 2550, C276)	Alloy (28, 825, 2550, C276)	Nickel Alloy SM2535, Nickle Alloy SM2242

Based on this study, the Nickel Alloy SM2535 or SM2242 (3% Mo) was the most appropriate choice of tubing material to be used. This was because the Nippon steel selection chart (Figure 18) was more technically and economically detailed. In terms of technical matters, this chart divided several materials into specific parameter values (partial pressure of CO_2 and H_2S, as well as temperature), which were adjusted to the economy.

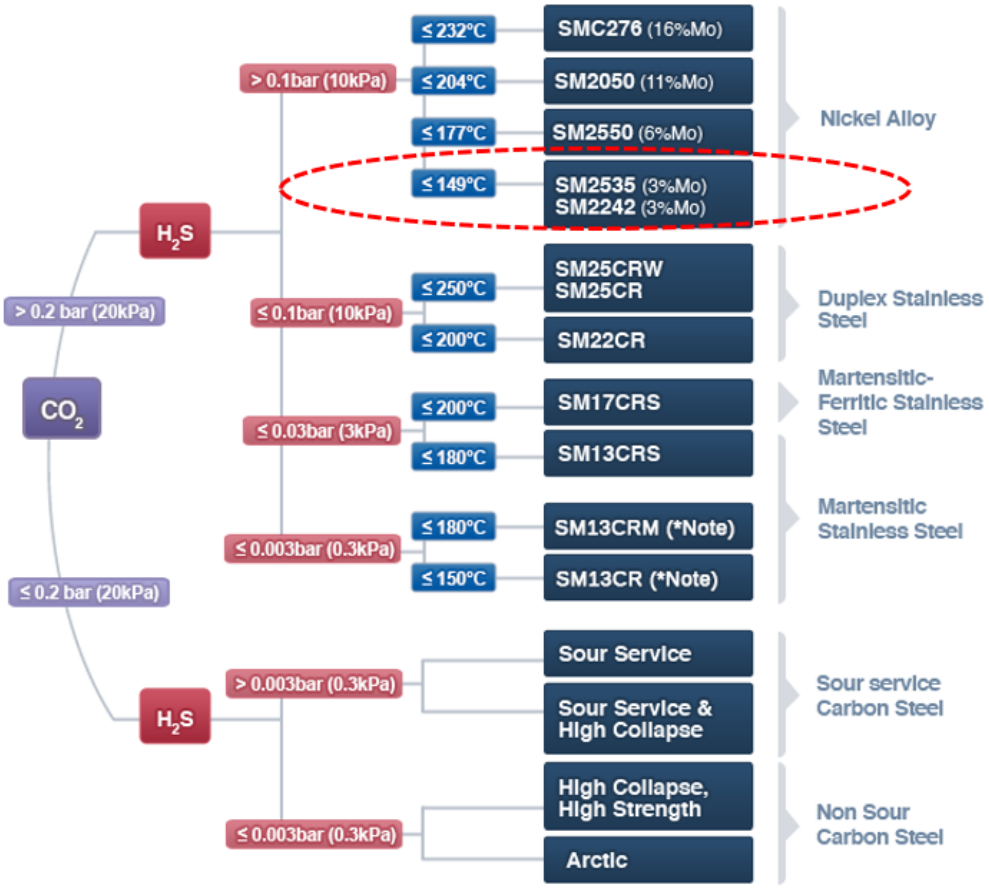

Source: http://www.tubular.nipponsteel.com/product-services/octg/materials/materials

Figure 18. Nippon steel chart for material selection

Nickel is an ideal base for corrosion-resistant alloys, due to being inherently resistant to certain chemicals. Also, it is highly alloyed with several elements known to enhance corrosion performance, such as chromium, copper, and molybdenum (Crook & Caron, 2014). Meanwhile, SM2535 and SM2242 are Austenitic Fe and Ni (Iron and Nickel) materials required for critical well conditions, each combining high concentrations of CO_2, H_2S, and chlorides (Fig 19 and 20), respectively.

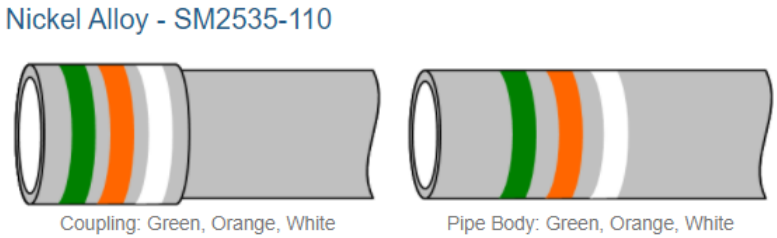

Source: http://www.tubular.nipponsteel.com/product-services/octg/materials/data-sheet/sm2535-110
(SM2535 is manufactured based on API 5CT / ISO 11960 and API 5CRA / ISO 13680)

Figure 19. Nickel Alloy SM2535

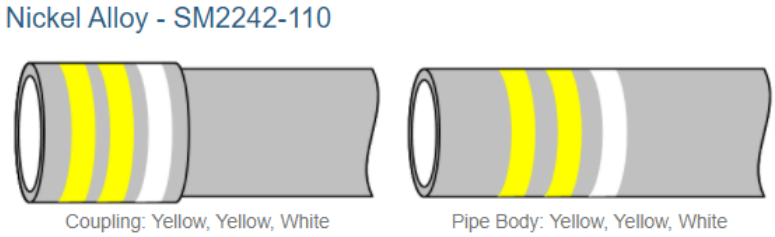

Source: http://www.tubular.nipponsteel.com/product-services/octg/materials/data-sheet/sm2242-110
(SM2242 is manufactured based on API 5CT / ISO 11960 and API 5CRA / ISO 13680)

Figure 20. Nickel Alloy SM2242

CONCLUSION

1. There were two corrosion agents in the X-well, namely carbon dioxide (CO_2) and hydrogen sulfide (H_2S).
2. Considering the diagram phase of fluid, the plan design of the X-field should be performed within the wet gas reservoir.
3. Based on the production forecast, the maximum produced gas rate was 56.648 MMSCFD. The optimum production rate also ranged from 17.89 to 41.754 MMSCFD, with an operating point of 19.1063 MMSCFD.
4. There was also damage in form of corrosion (0.46 mm/year) and pitting (4.5 mm/year). However, the corrosion rate was still in the allowance standards with sour service application (Region 3).
5. The ideal tubing material was Nickel Alloy SM2535 or SM2242, with conditions of high CO_2 and H_2S concentrations.

Recommendation

1. The integration of tubing material selection should be performed using economic calculation.
2. The considered cost should also determine the appropriate material for the condition besides the technical aspect. Moreover, the optimum production range should use calculations based on a formula, to show the real production plan for the well.
3. The technical feasibility study of another corrosion mitigation should also be considered to decrease technical risk and improve future operational effectiveness, such as inhibitor applications, use of protective coatings, and adequate monitoring and inspection.

REFERENCES

Boschee, P. (2014). Taking on the technical challenges of sour gas processing. *Oil and Gas Facilities*, *3*(06), 21–25.

Crook, P., & Caron, J. L. (2014). A study of the corrosion properties of welds and heat-affected zones of a wrought nickel alloy containing high levels of chromium and molybdenum. *NACE - International Corrosion Conference Series*.

Dr. Fatih Birol. (2019). World Energy Outlook 2019 ㅗ. *World Energy Outlook Sereies*.

Journal of Earth Energy Engineering
Vol. 11 No. 1, March 2022, pp 34-51

Dugstad, A., Lunde, L., & Videm, K. (1994). Parametric study of CO_2 corrosion of carbon steel. In *Corrosion*. NACE International, Houston, TX (United States).

Kilstrom, K. J. (1983). Whitney Canyon sour gas well completion techniques. *Journal of Petroleum Technology*, *35*(01), 40–46.

Lawrence, J. J., & Gupta, D. K. (2009). Quality assessment and consistency evaluation of hydrocarbon PVT data. *IPTC 2009: International Petroleum Technology Conference*, cp-151.

Norsok, T., & Industries, N. M. (2002). NORSOK STANDARD Materials selection. *NORSOK Standard Journal*, *6*(August), 9–11.

Popoola, L. T., Grema, A. S., Latinwo, G. K., Gutti, B., & Balogun, A. S. (2013). Corrosion problems during oil and gas production and its mitigation. *International Journal of Industrial Chemistry*, *4*(1), 1–15.

Pots, B. F. M., John, R. C., Rippon, I. J., Thomas, M. J. J. S., Kapusta, S. D., Girgis, M. M., & Whitham, T. (2002a). *Improvement on De Waard-Milliams Corrosion Prediction and Applications to Corrosion Management*. *02235*, 1–19.

Pots, B. F. M., John, R. C., Rippon, I. J., Thomas, M. J. J. S., Kapusta, S. D., Girgis, M. M., & Whitham, T. (2002b). Improvements on de waard-milliams corrosion prediction and applications to corrosion management. *NACE - International Corrosion Conference Series*, *2002-April*.

Smith, L. (1999). Control of corrosion in oil and gas production tubing. *British Corrosion Journal*, *34*(4), 247–253.